Calculation of gyrotropy coefficients in media with low-pitch helical structures

H. Dhaouadi,* F. Trabelsi, O. Riahi, and T. Othman
Université Tunis El-Manar, Faculté des Sciences de Tunis, Laboratoire de Physique de la Matière Molle et de Modélisation Électromagnétique (LP3ME), Campus Universitaire Farhat Hached 2092 Tunis, Tunisia

(Received 3 January 2018; published 25 April 2018)

Chiral smectic liquid crystals are known for their huge optical activity due to the precession of the anisotropic dielectric tensor around the helicoidal axis. For an oblique direction of the propagating wave, the helix acts as a grating which splits an incident beam in different directions as long as the pitch is not too small with respect to the light wavelength. When the pitch of the helix is smaller than the wavelength, the effect of the helix is a renormalization of the gyrotropic coefficients ($g_\perp$ and $g_\parallel$) of the resulting uniaxial medium. We report here on a method to compute these coefficients in that limit. Resolution of the Maxwell equations, using a perturbative approach, gives expressions for $g_\perp$ and $g_\parallel$ as a power development of the ratio ($\frac{p}{\lambda}$). The various terms of these developments coincide with the approximate expressions of these coefficients known in the literature.

DOI: 10.1103/PhysRevE.97.042704

I. INTRODUCTION

Natural optical activity is usually associated with molecules, or arrangement of molecules, having a helical structure. Pasteur argued that the optical activity of natural substances comes from atomic arrangements inside the molecules that differ from their mirror image (chiral materials) [1]. Chiral liquid crystals and, in particular, cholesteric and chiral smectic liquid crystals, offer a remarkable macroscopic model of the microscopic helical structure of chiral molecules [2–4]. Interest in the optics of anisotropic media has grown recently due to their importance in active and passive devices such as retarders, tunable filters, light modulators, optical disks, and displays [5,6].

More generally, it can be shown that optical activity arises from spatial inhomogeneities with atomic distances that are small with respect to the light wavelength. It is the case of the optical activity of noncentrosymmetric metals [7,8] and those of the so-called Weyl semimetals [9]. The breaking of degeneracy between left and right circularly polarized light in such media gives rise to phenomena such as the rotation of polarization with propagation (Faraday effect and optical activity) and upon reflection (Kerr effect) [10].

Such inhomogeneities give rise to an imaginary antisymmetric contribution to the dielectric tensor that displays spatial dispersion, i.e., depends on the light wave vector, or, equivalently, on the gradients of the electric field. This imaginary part is responsible for the rotatory power, and can be described in terms of a second-rank gyration pseudotensor γ_{ijk}.

The calculation of the light reflection, propagation, and transmission properties of these devices is essential to the design and understanding of the physics involved. This is also of great importance for the interpretation of experimental data from crystals and anisotropic structures using different optical techniques [11,12].

Several theoretical approaches exist for this purpose [13–15]. We report here on a method to compute the coefficients of the pseudotensor γ_{ijk} in the case of a chiral smectic liquid crystal presenting the Sm-C^*_α phase where the pitch of the helix is smaller than the wavelength.

In chiral smectic liquid crystals, optical activity is often introduced as a consequence of the nonlocal character of the dielectric tensor in chiral materials. In other words the electric displacement $\vec{D}$ contains the usual term proportional to the electric field $\vec{E}$ but also a term proportional to some gradient of the field whose coefficient is only allowed in the presence of chirality, due to the molecules in general but sometimes to the wound structure like in quartz (SiO_2) [16]. The order of magnitude of the optical rotatory power (ORP) due to gyrotropy is of some degrees of angle per decimeter [17].

In chiral liquid crystals, some phases like cholesteric or smectic C^* are locally anisotropic and gyrotropic and give rise to huge optical activity because the local axes are subject to a helicoidal precession around a direction of space. For large helical periods (pitches) of a few micrometers in the so-called Mauguin limit, the light polarization locks in with the rotating anisotropic axes so that the ORP is exactly 360° per pitch length for light propagating in the helix direction [18,19]. For smaller pitches, the rotation is not so large but still much larger than the "ordinary" gyrotropy as it reaches easily some tens of degrees per millimeter, so the intrinsic gyrotropy is often neglected in these systems [20]. When the pitch is of the order of the wavelength of light propagating in the material, one gets a selective reflection of circularly polarized light [18,19]. When the pitch gets smaller than the wavelength, it has been proposed by Oldano and Ratjeri [21], Galatola [22], and Etxebarria *et al.* [23] that the effect of the helix is to renormalize the gyrotropic coefficients of the material that becomes uniaxial around the helix axis. We will recall in the next section the known results about light propagation in such systems in the large pitch limit and in the gyrotropic limit. The following section will be devoted to the calculation of renormalized gyrotropic coefficients.

*hassen.dhaouadi@ipeit.rnu.tn

A. Chiral anisotropic media

1. Anisotropic chiral phase with a helicoidal precession of axes around z

The local dielectric tensor is such that

$$D_i(\vec{r}) = \varepsilon_{\rm ij}^{\rm eff}(\vec{r})\, E_j(\vec{r}). \tag{1}$$

When written in an axes frame where z is fixed, one gets z-dependent terms, $p = \frac{2\pi}{q}$ being the pitch of the helix:

$$\varepsilon_{\rm ij}^{\rm eff}(\vec{r}) = \bar{\varepsilon}\ \delta_{\rm ij} + \sum_{m=-2,+2} \varepsilon^m \exp(imqz)\ T_{\rm ij}^m, \tag{2}$$

where the following basis containing three elementary modes has been used [9]:

$$T_{\rm ij}^0 = \begin{pmatrix} -1 & 0 & 0 \\ 0 & -1 & 0 \\ 0 & 0 & 2 \end{pmatrix}, \quad T_{\rm ij}^{\pm 1} = \begin{pmatrix} 0 & 0 & 1 \\ 0 & 0 & \mp i \\ 1 & \mp i & 0 \end{pmatrix},$$
$$T_{\rm ij}^{\pm 2} = \begin{pmatrix} 1 & \mp i & 0 \\ \mp i & -1 & 0 \\ 0 & 0 & 0 \end{pmatrix}. \tag{3}$$

For a uniaxial material ($\varepsilon_\parallel$, $\varepsilon_\perp$, $\varepsilon_{\rm a} = \varepsilon_\parallel - \varepsilon_\perp$) tilted by an angle θ around y at $z = 0$, one gets

$$\bar{\varepsilon} = \frac{\varepsilon_\parallel + 2\varepsilon_\perp}{3}, \quad \varepsilon^0 = \frac{\varepsilon_a}{2}\left(\cos^2\theta - \frac{1}{3}\right),$$
$$\varepsilon^{\pm 1} = \frac{\varepsilon_a}{2}\sin\theta\cos\theta, \quad \text{and} \quad \varepsilon^{\pm 2} = \frac{\varepsilon_a}{4}\sin^2\theta. \tag{4}$$

This may represent in first approximation the synclinic SmC^* structure with layers parallel to the xy plane or, with $\theta = \frac{\pi}{2}$, a cholesteric whose director is along x at $z = 0$. One can split ε in two parts, the mean uniaxial component and the rotating one:

$$\varepsilon_{\rm ij}^{\rm eff}(\vec{r}) = \tilde{\varepsilon}_{\rm ij} + \Lambda_{\rm ij}(z), \tag{5}$$

with $\tilde{\varepsilon}_\perp = \bar{\varepsilon} - \varepsilon^0$, $\tilde{\varepsilon}_\parallel = \bar{\varepsilon} - 2\,\varepsilon^0$, and

$$\Lambda_{\rm ij}(z) = 2\,\varepsilon^1 \begin{pmatrix} 0 & 0 & \cos(qz) \\ 0 & 0 & \sin(qz) \\ \cos(qz) & \sin(qz) & 0 \end{pmatrix}$$
$$+2\,\varepsilon^2 \begin{pmatrix} \cos(2qz) & \sin(2qz) & 0 \\ \sin(2qz) & -\cos(2qz) & 0 \\ 0 & 0 & 0 \end{pmatrix}. \tag{6}$$

2. Anisotropic chiral phase with fixed axes

Following the notations of Landau *et al.* [16] and calculation carried out by Agranovich and Ginsbourg [24], one writes down $\vec{D}$ in a nonlocal form:

$$D_i = \varepsilon_{ik}\, E_k + \gamma_{ijk}\, \partial_j E_k. \tag{7}$$

There is no reason why γ_{ijk} should be a constant intrinsic to the material; it may depend on the wavelength of light like the corresponding pseudoscalar γ in chiral isotropic liquids that may give rise to circular dichroism. So, assuming a monochromatic light with wave vector k_0 in vacuum is at the origin of the field gradient, it is of common use in a uniaxial material to write down γ_{ijk} as

$$k_0\, \gamma_{ijk} = e_{ilk}\, g_{lj}, \tag{8}$$

where the gyrotropic tensor g_{lj} has two characteristic coefficients $g_\perp$ and $g_\parallel$ while e_{ilk} is the fully antisymmetric Levi-Civita tensor whose elements are nonzero only when i, l, and k are all different [25]. One gets explicitly in the axes frame, where z is the optical axis,

$$k_0\gamma_{xyz} = -k_0\,\gamma_{zyx} = g_\perp, \quad k_0\gamma_{yzx} = -k_0\gamma_{xzy} = g_\parallel, \quad \text{and}$$
$$k_0\gamma_{zxy} = -k_0\gamma_{yxz} = g_\perp. \tag{9}$$

3. Connection between the two regimes: the low-pitch limit

First let us remark that we should have combined the two contributions in the case of precessing axes, introducing a mean gyrotropic tensor and a rotating one developed on the same basis. Anyway one does neglect the gyrotropy in that case due to the much smaller order of magnitude of the associated rotatory power. We are more interested, following the work of Oldano and Ratjeri [21], in computing the renormalized gyrotropy coefficients obtained when the pitch of a precessing system becomes much smaller than the light wavelength. This leads to an effective uniaxial gyrotropic system. We will first recall how the light plane waves propagate in such materials before computing the low-pitch limit with a perturbative approach.

B. Light propagation

1. Propagation along the helix

In that case, an exact solution was derived long ago by de Vries [13] for light propagating in a cholesteric liquid crystal. It can be generalized to tilted smectics [26]. The main features are that the eigenmodes for the displacement $\vec{D}$ consist of two pairs ($i = 1, 2$) of circularly polarized plane waves D_i^+, D_i^- with a wave vector difference $k_i^+ - k_i^- = \pm 2q$ and an amplitude ratio $\frac{D_i^+}{D_i^-}$ depending strongly on the pitch-to-wavelength ratio $\frac{p}{\lambda}$. For large pitches, in the Mauguin limit, two ordinary circular waves with $\overrightarrow{k} = \vec{k}_o \pm \overrightarrow{q}$ and the same amplitude form one mode while two extraordinary ones with $\overrightarrow{k} = \vec{k}_e \pm \overrightarrow{q}$ form the second mode. The final state of polarization will depend on the boundary conditions at the entrance; for example, a wave which is purely ordinary (or purely extraordinary) will have its polarization rotated by 360° per pitch length in the sample. This effect is widely used in twisted nematics (TN) displays. When the pitch gets smaller, the amplitude ratios inside each pair become very different from unity so that the right circular polarization dominates one mode and the left one dominates the second one. If the incoming wave is linearly polarized, the two leading circular modes have the same amplitude and a slightly different wave vector. This difference is at the origin of the ORP which obeys the de Vries formula:

$$\rho = \frac{\pi\, p^3 \Lambda_2^2}{\lambda^2(n^2 p^2 - \lambda^2)}. \tag{10}$$

We have used in this equation the notations previously defined in Sec. II; p is the pitch, λ the light wavelength in vacuum, $\Lambda_2 = 2\varepsilon$ the coefficient of the half-pitch modulation of ε, and n is an average index in the uniaxial resulting material. The de Vries equation is commonly used to describe the ORP in cholesterics and tilted smectics except in the Mauguin limit. It predicts $\rho \approx \frac{p}{\lambda^2}$ for large pitch, $\rho = \frac{p^3}{\lambda^4}$ at small pitch, and a divergence at $np = \lambda$ where the selective reflection of one particular circular wave takes place [18,19]. In this paper, we focus mainly on the small pitch limit where the validity of the precessing dielectric tensor can be questioned if the period is smaller than the optical wavelength.

2. *Propagation at angle with the helix: perturbative approach*

In the case when the pitch is large enough, the helix acts as a grating that induces transfers of wave vectors $\pm q$, $\pm 2q$ between the propagating waves. There is no simple solution with a finite set of modes like in the previous case but experimentally the existence of the grating has been shown and the selective reflection has been proven [11]. It was an elegant way to prove the difference of structure between the Sm-C^* phase, with Λ_1 and Λ_2 terms and two different selective reflections when $\vec{q}$ and $2\vec{q}$ satisfy the Bragg relation, and the Sm-C_A^* phase where only Λ_2 and $2\vec{q}$ exist and induce one selective reflection.

The main goal is to demonstrate that when the pitch of the helix is shorter than the light wavelength the medium behaves as uniaxial with a gyrotropy coefficient due to the effect of $\Lambda_{ij}(z)$. According to the method of Bensimon *et al.* [27], in the blue phases, it is considered that the electric field of the light wave is propagated with a wave vector k which forms an angle α with z. This field is decomposed in two parts, a part E^0 propagating normally in the uniaxial medium by creating a small perturbation E^1, due to the helicoidal structure.

One has thus to start:

$$D_i(\vec{r}) = [\tilde{\varepsilon}_{ij} + \Lambda_{ij}(z)]\big(E_j^0 + E_j^1\big)(\vec{r}). \tag{11}$$

The electromagnetic field propagation obeys the Maxwell equations:

$$\Delta\vec{E} - \vec{\nabla}(\mathrm{div}\vec{E}) - \frac{1}{c^2}\frac{\partial^2\vec{D}}{\partial t^2} = 0. \tag{12}$$

We assumed that the perturbation E_i^1 is created by $\Lambda_{ij}E_j^0$ and that $\Lambda_{ij}E_j^1$ is negligible.

$$\Delta(\vec{E}^0 + \vec{E}^1)_i - \nabla_i[\mathrm{div}(\vec{E}^0 + \vec{E}^1)] - \frac{1}{c^2}\frac{\partial^2}{\partial t^2}\big[\tilde{\varepsilon}_{ij}\big(E_j^0 + E_j^1\big) + \Lambda_{ij}(\mathrm{z})E_j^0\big] = 0 \tag{13}$$

One can separate the equations of evolution of E^0 and E^1, first the equation that governs the propagation of E^0 in a uniaxial medium:

$$\Delta(\vec{E}^0)_i - \nabla_i[\mathrm{div}(\vec{E}^0)] - \frac{1}{c^2}\frac{\partial^2}{\partial t^2}\big(\tilde{\varepsilon}_{ij}E_j^0\big) = 0. \tag{14}$$

Then the second one describes the propagation of E^1 created by the action of the helix on $\vec{E}^0$:

$$\Delta(\vec{E}^1)_i - \nabla_i[\mathrm{div}(\vec{E}^1)] - \frac{1}{c^2}\frac{\partial^2\big(\tilde{\varepsilon}_{ij}E_j^1\big)}{\partial t^2} = \frac{1}{c^2}\frac{\partial^2\big(\Lambda_{ij}(\mathrm{z})E_j^0\big)}{\partial t^2}. \tag{15}$$

We search to propagate a plane wave with $\exp(iwt)$; then $\frac{\partial^2}{\partial t^2}$ became $-w^2$ and we take the Fourier transformation of Eq. (15):

$$M_{ij}(\vec{q})E_j^1(\vec{q}) = \left(-q^2\delta_{ij} + q_iq_j + \frac{\omega^2}{c^2}\tilde{\varepsilon}_{ij}\right)E_j^1(\vec{q}) = -\frac{\omega^2}{c^2}\cdot\mathcal{F}\big(\Lambda_{ij}E_j^0\big)(\vec{q}). \tag{16}$$

where $M_{ij}(\vec{q})$ is a 3×3 matrix that inverses $M_{ki}^{-1}(\vec{q})$, such that $M_{ki}^{-1}M_{ij}(\vec{q}) = \delta_{kj}$, to obtain the following equation:

$$E_k^1(\vec{q}) = -\frac{\omega^2}{c^2}M_{ki}^{-1}(\vec{q})\cdot\mathcal{F}\big(\Lambda_{ij}E_j^0\big)(\vec{q}). \tag{17}$$

The reversed Fourier transformation of Eq. (17) gives

$$E_k^1(\vec{r}) = -\frac{\omega^2}{c^2}\int d^3r' M_{ki}^{-1}(\vec{r}-\vec{r}')\cdot\Lambda_{ij}(\mathrm{z}')E_j^0(\vec{r}'). \tag{18}$$

The field $E^1(\vec{r})$ is obtained by integration of $\Lambda(z')E^0(\vec{r}')$ around $\overrightarrow{r}$. It will be necessary to develop $E^0(\vec{r}')$ around $\overrightarrow{r}$ to reveal the field gradient and then the gyrotropy.

$$E_k^0(\vec{r}') \approx E_j^0(\vec{r}) + (r_m' - r_m)\frac{\partial E_j^0(\vec{r})}{\partial r_m}. \tag{19}$$

We must firstly reverse $M_{ij}(\vec{q})$ to calculate $M_{ij}^{-1}(\vec{q})$. We write M_{ij} as a matrix in the space $\vec{q}$ and we calculate its determinant Δ and then the matrix of cofactors. We introduce the ordinary and extraordinary optical wave vectors such as $k_\perp^2 = (\frac{\omega^2}{c^2})\tilde{\varepsilon}_\perp$ and $k_\parallel^2 = (\frac{\omega^2}{c^2})\tilde{\varepsilon}_\parallel$ which gives in the particular frame where z is the normal to the layers:

$$M_{ij}(\vec{q}) = \begin{pmatrix} k_\perp^2 - q_y^2 - q_z^2 & q_xq_y & q_xq_z \\ q_xq_y & k_\perp^2 - q_z^2 - q_x^2 & q_yq_z \\ q_xq_z & q_yq_z & k_\parallel^2 - q_y^2 - q_x^2 \end{pmatrix}. \tag{20}$$

The determinant is

$$\Delta = \big(k_\perp^2 - q^2\big)\big(k_\parallel^2k_\perp^2 - k_\parallel^2q_z^2 - k_\perp^2q_\perp^2\big). \tag{21}$$

Here we recognize the roots of the polynomial in q which give the ordinary and extraordinary wave vectors of a uniaxial medium.

The elements of $M_{ij}^{-1}(\vec{q})$ are written in the particular frame where z is the normal to the smectic layers ($q_\perp^2 = q_x^2 + q_y^2$ and $q^2 = q_\perp^2 + q_z^2$):

$$M_{xx}^{-1}(\vec{q}) = \frac{\big(k_\perp^2 - q_z^2 - q_x^2\big)\big(k_\parallel^2 - q_\perp^2\big) - q_y^2q_z^2}{\big(k_\perp^2 - q^2\big)\big(k_\parallel^2k_\perp^2 - k_\parallel^2q_z^2 - k_\perp^2q_\perp^2\big)}, \tag{22}$$

$$M_{yy}^{-1}(\vec{q}) = \frac{\big(k_\perp^2 - q_z^2 - q_y^2\big)\big(k_\parallel^2 - q_\perp^2\big) - q_x^2q_z^2}{\big(k_\perp^2 - q^2\big)\big(k_\parallel^2k_\perp^2 - k_\parallel^2q_z^2 - k_\perp^2q_\perp^2\big)}, \tag{23}$$

$$M_{zz}^{-1}(\vec{q}) = \frac{\left(k_\perp^2 - q_z^2\right)}{\left(k_\parallel^2 k_\perp^2 - k_\parallel^2 q_z^2 - k_\perp^2 q_\perp^2\right)}, \tag{24}$$

$$M_{yx}^{-1}(\vec{q}) = M_{xy}^{-1}(\vec{q}) = \frac{-q_x q_y\left(k_\parallel^2 - q^2\right)}{\left(k_\perp^2 - q^2\right)\left(k_\parallel^2 k_\perp^2 - k_\parallel^2 q_z^2 - k_\perp^2 q_\perp^2\right)}, \tag{25}$$

$$M_{xz}^{-1}(\vec{q}) = M_{zx}^{-1}(\vec{q}) = \frac{-q_x q_z}{\left(k_\parallel^2 k_\perp^2 - k_\parallel^2 q_z^2 - k_\perp^2 q_\perp^2\right)}, \tag{26}$$

$$M_{yz}^{-1}(\vec{q}) = M_{zy}^{-1}(\vec{q}) = \frac{-q_y q_z}{\left(k_\parallel^2 k_\perp^2 - k_\parallel^2 q_z^2 - k_\perp^2 q_\perp^2\right)}. \tag{27}$$

Once the $M_{ij}^{-1}(\vec{q})$ is known, we can calculate the inverse Fourier transform $M_{ij}^{-1}(\vec{r} - \vec{r}')$ and replace it in Eq. (18); we do not need to calculate all terms, only those certain to be used in the computing of gyrotropy.

One takes again the calculation of $\vec{D}(\vec{r})$ in Eq. (11) which becomes locally (all tensors are in the particular axes where z is normal to layers)

$$D_l(\vec{r}) = \left[\tilde{\varepsilon}_{lk} E_k(\vec{r}) + \Lambda_{lk} E_k^0(\vec{r})\right] - \left(\frac{\omega}{c}\right)^2 \int d^3 r' \Lambda_{lk}(z) \times M_{ki}^{-1}(\vec{r} - \vec{r}') \Lambda_{ij}(z') E_j^0(\vec{r}'). \tag{28}$$

We use the hypothesis that the pitch p is shorter than the wavelength λ; then the second term is eliminated if one averages $\vec{D}$ over a small length in front of λ.

One rewrites Eq. (28) as follows:

$$D_l(\vec{r}) = \tilde{\varepsilon}_{lk} E_k(\vec{r}) - \left(\frac{\omega}{c}\right)^2 \left[\int d^3 r' \Lambda_{lm}(z) \cdot M_{mi}^{-1}(\vec{r} - \vec{r}') \cdot \Lambda_{ik}(z') \cdot (r_j' - r_j)\right] \frac{\partial E_k^0(\vec{r})}{\partial r_j}. \tag{29}$$

One finds finally the gyrotropy:

$$\gamma_{ljk}(\vec{r}) = -\left(\frac{\omega}{c}\right)^2 \left[\int d^3 r' \Lambda_{lm}(z) \cdot M_{mi}^{-1}(\vec{r} - \vec{r}') \cdot \Lambda_{ik}(z') \cdot (r_j' - r_j)\right]. \tag{30}$$

If one manages to show that the function to be integrated depends only on $(\vec{r}' - \vec{r}) = \vec{\rho}$, it will come that γ_{ljk} does not depend on $\overrightarrow{r}$ and one will be able to calculate the required *gyrotropy* coefficients thereafter. For that it is necessary to carry out the matrix product $\Gamma_{lk} = \Lambda_{lm}(z) M_{mi}^{-1}(\vec{r} - \vec{r}') \Lambda_{ik}(z')$. Knowing that elements of matrix Λ_1 are in $\cos(qz)$ and those of Λ_2 are in $\cos(2qz)$, one will have, finally, terms with $\cos q(z \pm z')$. The terms in $(z–z')$ are to be kept and the others to be removed because $M_{mi}^{-1}(\vec{r} - \vec{r}')$ must be maximum for $\vec{r} = \vec{r}'$.

It is necessary to calculate Γ_{lk}^1 and Γ_{lk}^2 elements of the matrix.

$$\Gamma^1 = (\Lambda_1)^2 \begin{pmatrix} 0 & 0 & \cos(qz) \\ 0 & 0 & \sin(qz) \\ \cos(qz) & \sin(qz) & 0 \end{pmatrix} \times M^{-1}(\vec{r} - \vec{r}') \begin{pmatrix} 0 & 0 & \cos(qz') \\ 0 & 0 & \sin(qz') \\ \cos(qz') & \sin(qz') & 0 \end{pmatrix}, \tag{31}$$

$$\Gamma^2 = (\Lambda_2)^2 \begin{pmatrix} \cos(2qz) & \sin(2qz) & 0 \\ \sin(2qz) & -\cos(2qz) & 0 \\ 0 & 0 & 0 \end{pmatrix} \times M^{-1}(\vec{r} - \vec{r}') \begin{pmatrix} \cos(2qz') & \sin(2qz') & 0 \\ \sin(2qz') & -\cos(2qz') & 0 \\ 0 & 0 & 0 \end{pmatrix}. \tag{32}$$

As one kept only the terms in (z′–z) in the matrix Γ, Eq. (30) does not depend any more on r after having carried out the integral over $\rho = (r' - r)$.

One will explicitly look at the terms of the tensor of gyrotropy being calculated:

$$\gamma_{lmk}(\vec{r}) = -\left(\frac{\omega}{c}\right)^2 \left[\int \Gamma_{lk}(\vec{\rho}) \rho_m d^3 \rho\right]. \tag{33}$$

If we note m_{ij} the matrix elements M_{ij}^{-1}, the diagonal terms $(l = k)$ are all null, indeed:

$$\gamma_{xmx} = -\frac{1}{2}\left(\frac{\omega}{c}\right)^2 \int \rho_m [m_{zz}(\Lambda_1)^2 \cos(q\rho_z) + (m_{xx} + m_{yy})(\Lambda_2)^2 \cos(2q\rho_z)] d^3\rho = 0, \tag{34}$$

because the function is odd in ρ_m.

Finally by eliminating all the even terms, there remain only two terms corresponding to $g_\perp$ and $g_\parallel$.

In what follows, we replaced $\frac{w^2}{c^2}$ by k_0^2.

$$\frac{g_\perp}{k_0} = \gamma_{xyz} = \gamma_{zxy} = -\gamma_{zyx} = -\gamma_{yxz} = -\frac{k_0^2}{2} \int \rho_y [m_{yz}(\Lambda_1)^2 \sin(q\rho_z)] d^3\rho = 0,$$

$$\frac{g_\parallel}{k_0} = \gamma_{xzy} = -\gamma_{yzx} = -\frac{k_0^2}{2} \int \rho_z [m_{zz}(\Lambda_1)^2 \sin(q\rho_z) + (m_{xx} + m_{yy})(\Lambda_2)^2 \sin(2q\rho_z)] d^3\rho. \tag{35}$$

C. Calculation of $g_\perp$

There are now only three integrals to calculate, the first giving $g_\perp$:

$$\int \rho_y [m_{yz} \sin(q\rho_z)] d^3\rho = 0, \tag{36}$$

for which we need initially the inverse of the Fourier transform:

$$m_{yz}(\vec{\rho}) = \frac{1}{8\pi^3} \int \frac{-q_y q_z \exp(i\vec{q} \cdot \vec{\rho})}{\left(k_\parallel^2 k_\perp^2 - k_\parallel^2 q_z^2 - k_\perp^2 q_\perp^2\right)} d^3 q, \tag{37}$$

$$m_{yz} = \frac{-k_\parallel^2 k_\perp \rho_y \rho_z \exp\left(i\sqrt{k_\parallel^2 \rho_\perp^2 + k_\perp^2 \rho_z^2}\right)}{4\pi\left(k_\parallel^2 \rho_\perp^2 + k_\perp^2 \rho_z^2\right)^{5/2}} \left[-\left(k_\parallel^2 \rho_\perp^2 + k_\perp^2 \rho_z^2\right) - 3i\sqrt{k_\parallel^2 \rho_\perp^2 + k_\perp^2 \rho_z^2} + 3\right]. \tag{38}$$

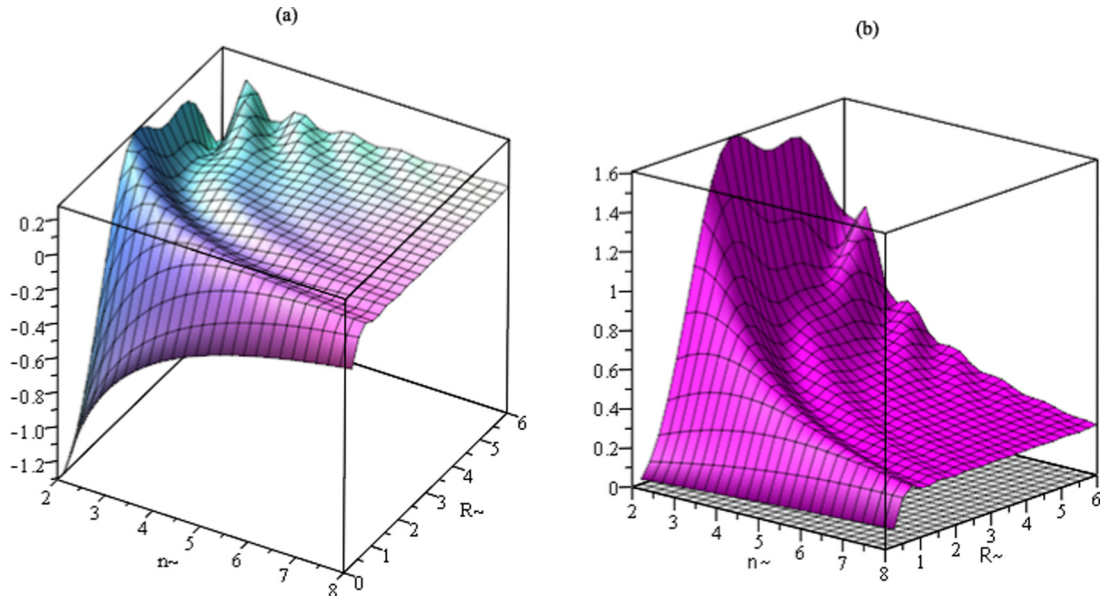

FIG. 1. Representation of the real part of the function of the integral [Eq. (44)] (a) and of the primitive $I(\tilde{n},\tilde{R})$ (b). We see that for $\tilde{R} > 1$ the function is constant and positive; it depends only on $\tilde{n}$.

If we go back to $g_\perp$,

$$g_\perp = \frac{k_0^3 (\Lambda_1)^2}{8\pi} \int (k_\parallel \rho_y)^2 k_\perp \rho_z \sin(q\ \rho_z) \times \frac{\exp\left(i\sqrt{k_\parallel^2\rho_\perp^2 + k_\perp^2\rho_z^2}\right)}{\left(k_\parallel^2\rho_\perp^2 + k_\perp^2\rho_z^2\right)^{5/2}} \left[-\left(k_\parallel^2\rho_\perp^2 + k_\perp^2\rho_z^2\right) -3i\sqrt{k_\parallel^2\rho_\perp^2 + k_\perp^2\rho_z^2} + 3\right] d^3\rho. \quad (39)$$

In this expression, $\sin(q\rho_z)$ varies very quickly whereas the terms in $k\rho$ are close to zero and vary slowly. We continue the calculations in spherical coordinates $\widetilde{R}$, ϑ, and φ:

$$k_\parallel \rho_x = \tilde{R}\sin\vartheta\cos\varphi, \quad k_\parallel \rho_y = \tilde{R}\sin\vartheta\sin\varphi, \quad k_\perp \rho_z = \tilde{R}\cos\vartheta. \quad (40)$$

φ varies from 0 to 2π, ϑ from 0 to π, and ρ from 0 to a fraction of the wavelength of light (or a fraction of a micron since it is the length on which one defines the macroscopic quantities as ε_{ij} or g_{ij}). Therefore $\tilde{R}$ varies from 0 to π; on the other hand because of the parity of the function we integrate

$$g_\perp = \frac{k_0^3 (\Lambda_1)^2}{8\pi k_\parallel^2 k_\perp} \int_0^{\sim\pi} d\widetilde{R} \int_0^{\frac{\pi}{2}} \sin\varphi^2 d\varphi, \int_0^{\frac{\pi}{2}} \sin\vartheta^3 \cos\vartheta \sin\left(\frac{q}{k_\perp}\widetilde{R}\cos\vartheta\right) \exp^{i\tilde{R}}(-\tilde{R}^2 - 3i\tilde{R} + 3) d\vartheta. \quad (41)$$

We carry out the integral on φ:

$$g_\perp = \frac{k_0^3 (\Lambda_1)^2}{8\pi k_\parallel^2 k_\perp} \int_0^{\frac{\pi}{2}} \sin\vartheta^3 \cos\vartheta\ d\vartheta \int_0^{\sim\pi} \sin\left(\frac{q}{k_\perp}\tilde{R}\cos\vartheta\right) \times \exp^{i\tilde{R}}(-\tilde{R}^2 - 3i\tilde{R} + 3) d\tilde{R}. \quad (42)$$

The integral on ϑ gives (with $A = \frac{q}{k_\perp}\tilde{R} = \tilde{n}\tilde{R}$ and by taking the notations of Appendix C)

$$\int_0^{\frac{\pi}{2}} \sin\vartheta^3 \cos\vartheta\ \sin(A\cos\vartheta) d\vartheta = -2\frac{A^2\sin A + 3A\cos A - 3\sin A}{A^4} = f^2(A) = f^2(\tilde{n}\tilde{R}). \quad (43)$$

We pass then to integration on $\tilde{R}$:

$$\int_0^{\sim\pi} \frac{-2\tilde{n}^2\tilde{R}^2\sin\tilde{n}\widetilde{R} + 3\tilde{n}\tilde{R}\cos\tilde{n}\tilde{R} - 3\sin\tilde{n}\tilde{R}}{\tilde{n}^4\tilde{R}^4} \times(-\tilde{R}^2 - 3i\tilde{R} + 3)\exp^{i\tilde{R}} d\tilde{R}. \quad (44)$$

The function of the integral (44) is integrable on MAPLE; its primitive can be put in the form

$$I(\tilde{n},\tilde{R}) = 2\exp^{i\tilde{R}}\left[\frac{i\sin(\tilde{n}\tilde{R}) - \tilde{n}\cos(\tilde{n}\tilde{R})}{\tilde{n}^2(\tilde{n}^2-1)} + \frac{3(1-i\tilde{R})[\tilde{n}\tilde{R}\cos(\tilde{n}\tilde{R})] - \sin(\tilde{n}\tilde{R})}{\tilde{n}^4\tilde{R}^4}\right]. \quad (45)$$

The representation of the real part of the function of the integral (44) shows oscillations around zero for the large values of $\tilde{n}$ and $\tilde{R}$ [Fig. 1(a)]. Representation of the real part of the primitive $I(\tilde{n},\tilde{R})$ shows that for $\tilde{R} > 1$ the function is constant and positive; it depends only on $\tilde{n}$ [Fig. 1(b)]. Fortunately, the upper limit of (the real part of) *the primitive* $I(\tilde{n},\tilde{R})$ is small (about 1.4×10^{-3} for $\tilde{R} = \pi$ and $\tilde{n} = 10$); then the lower limit, which is written as

$$\frac{-2\tilde{n}}{\tilde{n}^2 - 1}, \quad (46)$$

dominates (its value is -0.2 for $\tilde{n} = 10$).

To estimate our $g_\perp$ we take

$$\Lambda_1 = \varepsilon_a \sin\theta\cos\theta, \quad k_0 = \frac{2\pi}{\lambda}, \quad \tilde{n} = \frac{q}{k_\perp}, \quad k_\perp^2 = \tilde{\varepsilon}_\perp k_0^2,$$

$$\text{and} \quad k_\parallel^2 = \tilde{\varepsilon}_\parallel k_0^2 : g_\perp = \frac{\varepsilon_a^2}{8\tilde{\varepsilon}_\parallel}\sin(2\theta)^2 \frac{p/\lambda}{1-\tilde{\varepsilon}_\perp p^2/\lambda^2}. \quad (47)$$

If we return to the calculation of Oldano and Ratjeri [21], we find that the dominant term of $g_\perp$ was in $\frac{p}{\lambda}$.

$$g_\perp^{\text{Oldano}} = -\frac{p}{\lambda}\frac{\varepsilon_a^2}{8\tilde{\varepsilon}_e}\sin(2\theta)^2. \quad (48)$$

It is well the same formula (except for the sign) with a corrective term in powers of $(\frac{p}{\lambda})^2$. In conclusion, one finds the solution of Oldano and Ratjeri if one keeps only the term in $(\frac{p}{\lambda})$ in $g_\perp$ and one finds the limited development of Etxebarria *et al.* [23]. Moreover divergence of $g_\perp$ takes place for the selective reflexion ($\lambda = np$).

II. CALCULATION OF $g_\parallel$

According to Eq. (35) two integrals are to be calculated to obtain $g_\parallel$.

$$(\Lambda_1)^2 \int \rho_z (m_{zz}\sin q\rho_z) d^3\rho, \quad (49)$$

$$(\Lambda_2)^2 \int \rho_z [(m_{xx}+m_{yy})\sin 2q\rho_z] d^3\rho. \quad (50)$$

Calculation shows that there is no contribution of Λ_1 to $g_\parallel$. We try to calculate the contribution of Λ_2. We have the following:

$$(m_{xx}+m_{yy})(\vec{\rho}) = \frac{k_\parallel^2(k_\parallel^2-2k_\perp^2)}{k_\parallel^2-k_\perp^2} I_0 + 2\Delta_\perp I_0 - \frac{k_\parallel^2}{k_\parallel^2-k_\perp^2}\Delta I_0 + I_1 + \frac{\partial(\vec{\rho})}{k_\parallel^2-k_\perp^2}, \quad (51)$$

where I_1 is the inverse Fourier transform of $\frac{1}{k_\perp^2-q^2}$ (cf. Appendix A):

$$I_1(\vec{\rho}) = -\frac{\exp(ik_\perp\rho)}{4\pi\rho}. \quad (52)$$

we want to calculate:

$$g_\parallel = \frac{-k_0^3(\Lambda_2)^2}{2}\int \rho_z [(m_{xx}+m_{yy})\sin(2q\rho_z)] d^3\rho. \quad (53)$$

We found the following:

$$g_\parallel = -\frac{k_0^3(\Lambda_2)^2}{2}\left\{\int -\rho_z \sin(2q\rho_z)\frac{\exp^{i\tilde{R}}}{4\pi k_\perp \tilde{R}}\left[\frac{k_\parallel^2(k_\parallel^2-2k_\perp^2)}{k_\parallel^2-k_\perp^2}\right] d^3\rho + \int -\rho_z\sin(2q\rho_z)\frac{\exp^{i\tilde{R}}}{2\pi k_\perp} \times\left[2k_\parallel^2\left(+\frac{i}{\tilde{R}^2}-\frac{1}{\tilde{R}^3}\right)+k_\parallel^4\rho_\perp^2\left(-\frac{1}{\tilde{R}^3}-\frac{3i}{\tilde{R}^4}+\frac{3}{\tilde{R}^5}\right)\right] d^3\rho + \int \rho_z\sin(2q\rho_z)\frac{k_\parallel^2\exp^{i\tilde{R}}}{4\pi k_\perp(k_\parallel^2-k_\perp^2)} \times\left[(k_\parallel^2+k_\perp^2)\left(+\frac{i}{\tilde{R}^2}-\frac{1}{\tilde{R}^3}\right)+(k_\parallel^4\rho_\perp^2+k_\perp^4\rho_z^2)\left(-\frac{1}{\tilde{R}^3}+\frac{3i}{\tilde{R}^4}+\frac{3}{\tilde{R}^5}\right)\right] d^3\rho\right\} - \int \rho_z\sin(2q\rho_z)\frac{\exp(ik_\perp\rho)}{4\pi\rho} d^3\rho. \quad (54)$$

Note that the first term (with I_0) and the last (with I_1) are proportional. In fact, with the definition of $\tilde{\rho}$ given in Appendix A, we have $\frac{\exp^{(i\tilde{R})}}{4\pi k_\perp \tilde{R}} = \frac{1}{k_\perp^2}\frac{\exp^{(ik_\perp\tilde{\rho})}}{4\pi\tilde{\rho}}\frac{k_\perp^2}{k_\parallel^2} d^3\tilde{\rho}$.

We need three integrations after a few regroupings. We start with the first:

$$J_1 = \frac{k_0^3}{8\pi}\frac{2k_\parallel^2-3k_\perp^2}{k_\parallel^2-k_\perp^2}(\Lambda_2)^2\int \rho_z \sin(2q\rho_z)\frac{\exp^{(ik_\perp\rho)}}{\rho} d^3\rho. \quad (55)$$

We continue with the second:

$$J_2 = \frac{k_0^3 k_\parallel^2}{8\pi k_\perp}\frac{k_\parallel^2-5k_\parallel^2k_\perp^2}{k_\parallel^2-k_\perp^2}(\Lambda_2)^2\int \rho_z\sin(2q\rho_z) \times\exp^{i\tilde{R}}\left(+\frac{i}{\tilde{R}^2}-\frac{1}{\tilde{R}^3}\right) d^3\rho. \quad (56)$$

Finally we have

$$J_3 = \frac{k_0^3 k_\parallel^2}{8\pi k_\perp(k_\parallel^2-k_\perp^2)}(\Lambda_2)^2\int \rho_z\sin(2q\rho_z)\exp^{i\tilde{R}}\left[k_\parallel^2(k_\parallel^2 -2k_\perp^2)(\rho_\perp^2-k_\perp^4\rho_z^2)\left(-\frac{1}{\tilde{R}^3}-\frac{3i}{\tilde{R}^4}+\frac{3}{\tilde{R}^5}\right)\right] d^3\rho. \quad (57)$$

As before, we continue the calculations in spherical coordinates, the integration on φ gives 2π, and that on ϑ gives (twice)

$$f^1(\tilde{n},\tilde{R}) \text{ or } f^2(\tilde{n},\tilde{R}) \text{ or } f^3 = f^1 + f^2.$$

$$J_1 = \frac{k_0^3}{4k_\perp^3}\frac{2k_\parallel^2-3k_\perp^2}{k_\parallel^2-k_\perp^2}(\Lambda_2)^2\int_0^{R_m} f^1(\tilde{n},\tilde{R})\tilde{R}^2\exp^{i\tilde{R}} d\tilde{R}, \quad (58)$$

$$J_2 = \frac{k_0^3 k_\parallel^2}{4k_\perp^3}\frac{k_\parallel^2-3k_\perp^2}{k_\parallel^2-k_\perp^2}(\Lambda_2)^2\int_0^{R_m} f^1(\tilde{n},\tilde{R})(1+i\tilde{R})\exp^{i\tilde{R}} d\tilde{R}, \quad (59)$$

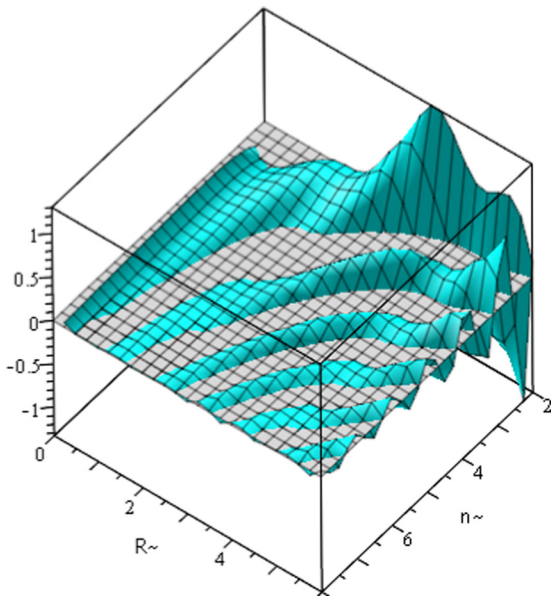

FIG. 2. Representation of the real part of the primitive I_1 of the function of the integral [Eq. (61)]. The upper limit oscillates around zero and the lower limit is dominant.

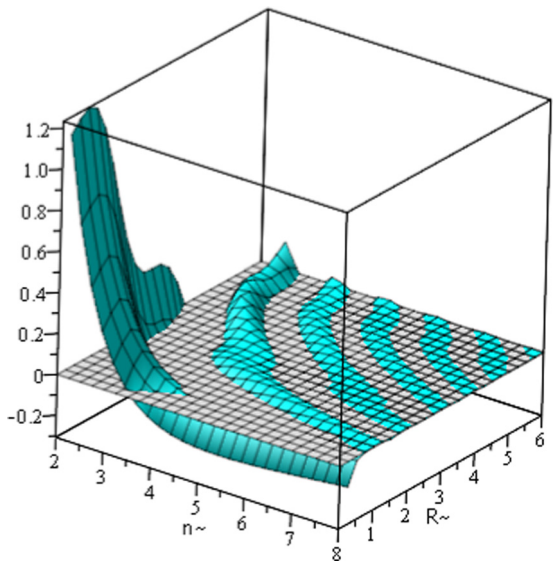

FIG. 3. Representation of the real part of the primitive I_2 of the function of the integral [Eq. (62)]. The upper limit oscillates around zero and the lower limit is dominant.

$$J_3^1 = -\frac{k_0^3 k_\perp^2}{4k_\perp^3\left(k_\parallel^2 - k_\perp^2\right)}(\Lambda_2)^2 \int_0^{R_m} f^1(\tilde{n},\tilde{R})(3 + 3i\tilde{R} - \tilde{R}^2) \times \exp^{i\tilde{R}} d\tilde{R}, \tag{60}$$

$$J_1 + J_2 + J_3^1 = \frac{k_0^3}{2k_\perp^3}(\Lambda_2)^2 \int_0^{R_m} f^1(\tilde{n},\tilde{R})(\tilde{R}^2 - i\tilde{R} - 1) \times \exp^{i\tilde{R}} d\tilde{R}, \tag{61}$$

$$J_3^2 = \frac{k_0^3}{4k_\perp^5}\left(k_\parallel^2 - k_\perp^2\right)(\Lambda_2)^2 \int_0^{R_m} f^2(\tilde{n},\tilde{R})(3 + 3i\tilde{R} - \tilde{R}^2) \times \exp^{i\tilde{R}} d\tilde{R}. \tag{62}$$

These two last expressions are integrable with MAPLE, but it is certainly more convenient for reasons of clearness to look at the representations of their primitives. In Fig. 2, (respectively, in Fig. 2), we present the primitive I_1, (respectively, I_2), of the function of the integral $J_1 + J_2 + J_3^1$ (respectively, J_3^2).

It is noticed that for the two integrals $I_1 = J_1 + J_2 + J_3^1$ and $I_2 = J_3^2$ the upper limits oscillate around zero and the lower limits are dominant (Figs. 2 and 3).

MAPLE calculations give

$$I_1(0) = \frac{\tilde{n}^5 - 5\tilde{n}^3 + 2\tilde{n} - (\tilde{n}^2 - 1)^2 \ln\left(\frac{|\tilde{n}+1|}{|\tilde{n}-1|}\right)}{\tilde{n}^2(\tilde{n}^2 - 1)^2}, \tag{63}$$

$$I_2(0) = \frac{-2\tilde{n}^5 + 18\tilde{n}^3 - 18\tilde{n} + 3(\tilde{n}^2 - 1)(\tilde{n}^2 - 3)\ln\left(\frac{|\tilde{n}+1|}{|\tilde{n}-1|}\right)}{\tilde{n}^4(\tilde{n}^2 - 1)^2}. \tag{64}$$

A development of $I_1(0)$ and $I_2(0)$, for $\tilde{n}$ large in front of 1, gives

$$I_1(0) \approx \frac{\tilde{n}^3 - 7\tilde{n}}{(\tilde{n}^2 - 1)^2} \quad \text{and} \quad I_2(0) \approx \frac{-2\tilde{n}^3 + 26\tilde{n}}{(\tilde{n}^2 - 1)^2}. \tag{65}$$

Finally, one finds by replacing the integrals $I_1(0)$ and $I_2(0)$ by their approached expressions in Eqs. (61) and (62), with, to recall, the following:

$$\Lambda_2 = \frac{1}{2}\varepsilon_a \sin(\theta)^2, \quad k_0 = \frac{2\pi}{\lambda}, \tilde{n} = \frac{q}{k_\perp},$$
$$k_\perp^2 = \tilde{\varepsilon}_\perp k_0^2, \quad \text{and} \quad k_\parallel^2 = \tilde{\varepsilon}_\parallel k_0^2.$$
$$g_\parallel \approx \frac{\varepsilon_a^2(2\tilde{\varepsilon}_\perp - \tilde{\varepsilon}_\parallel)}{8\tilde{\varepsilon}_\perp^2\left(1 - \tilde{\varepsilon}_\perp(p/\lambda)^2\right)^2}\sin^4(\theta)\left(\frac{p}{\lambda}\right) + \frac{\varepsilon_a^2(13\tilde{\varepsilon}_\parallel - 20\tilde{\varepsilon}_\perp)}{8\,\tilde{\varepsilon}_\perp(1 - \tilde{\varepsilon}_\perp(p/\lambda)^2)^2}\sin^4(\theta)\left(\frac{p}{\lambda}\right)^3. \tag{66}$$

This result for $g_\parallel$ is quite in conformity with the term of the ORP of de Vries which is in $(\frac{p}{\lambda})^3$ if the pitch p is higher than λ. Finally, since the term in $(\frac{p}{\lambda})^3$ is negligible for low pitch, we have

$$g_\parallel \approx \frac{\varepsilon_a^2(2\tilde{\varepsilon}_\perp - \tilde{\varepsilon}_\parallel)}{8\tilde{\varepsilon}_\perp^2\left[1 - \tilde{\varepsilon}_\perp(p/\lambda)^2\right]^2}\sin^4(\theta)\left(\frac{p}{\lambda}\right). \tag{67}$$

III. SUMMARY AND DISCUSSION

In this work we performed a calculation of gyrotropic coefficients $g_\parallel$ and $g_\perp$ in mediums with low-pitch helical structures (which corresponds to the phase Sm-C_α^* of a chiral smectic liquid crystal). These coefficients are directly related to the pitch of the helix and conform to experimental results [11,28]. The rigorous calculation we have done give better results than

those found in the literature. Indeed, the expressions found for $g_\perp$ and $g_\parallel$ are presented as a power development of the ratio $(\frac{p}{\lambda})$. The term of the first order of this development coincides with the results of Oldano and Ratjeri [21] and those of the third order $(\frac{p^3}{\lambda^3})$ coincide with the term of the optical rotation of de Vries which is $\frac{p^3}{\lambda^4}$ in the limit of small helical pitch [13]. Better still, with the found expressions one finds the selective reflections for a wavelength of the order of the pitch.

The calculation of orders of magnitude with $\varepsilon_\parallel \sim 3$, $\varepsilon_\perp \sim 2.5$, $\frac{p}{\lambda} \sim 0.1$, and $\theta = 10^\circ$ gives, respectively: $g_\parallel \sim 10^{-6}$ and $g_\perp \sim 10^{-4}$. If these orders of magnitude are correct, $g_\parallel$ is negligible in front of $g_\perp$, while being different from the de Vries term, and one must expect an ellipticity independent of the incident angle and close to 3×10^{-4}.

This confirm that the experimental results available are distorted by the use of no valid formulas, which give overestimated values of the ellipticity (as $g_\perp \sim 3 \times 10^{-3}$ and $\theta \sim 15^\circ$, for example) [23]. Moreover, the values of the ellipticity predicted are probably overestimated.

Experimental validation of the theoretical results obtained is necessary, but such an experimental work requires a chiral smectic liquid crystal that presents the Sm-C^*_α phase over a fairly wide temperature range, 2 °C–3 °C, minimum, and it is more difficult, still, to achieve well oriented homeotropic anchoring cells with thicknesses of the order of 100 μm. For these reasons we started an experimental work aiming at carrying out measurements of gyrotropic coefficients in the case of quartz. To do this, an alternative experimental method was used, consisting of a measurement of the ellipticity of the electromagnetic wave at the exit of the sample following an oblique propagation with respect to the axis of the helix. Measurements gave for $g_\parallel$ a value of $4.7717 \times 10^{-5} \pm 1.2771 \times 10^{-6}$ and for $\Delta g = g_\perp - g_\parallel$ a value of $7.4293 \times 10^{-5} \pm 5.5611 \times 10^{-6}$. The results obtained shall be published soon.

Experimental studies of chiral smectic liquid crystal are generally done by using SSFLC cells with planar anchoring [29]. In that case, the samples are produced with the helix axis parallel to the glass plates. Exact calculations of the optical properties are therefore particularly difficult, because the formalism of the Berreman matrix is no longer adequate to treat this particular geometry, and a more complex approach is needed [14]. In contrast, the calculation performed in this paper provides excellent results for all particular purposes (the perturbative approach to study the propagation at an angle with the helix).

APPENDIX A: FOURIER TRANSFORMS

We compute I_0 and I_1:

$$I_0(\vec{\rho}) = \frac{1}{8\pi^3}\int \frac{\exp(i\vec{q}\vec{\rho})}{k_\parallel^2 k_\perp^2 - k_\parallel^2 q_z^2 - k_\perp^2 q_\perp^2}, \quad I_1(\vec{\rho}) = \frac{1}{8\pi^3}\int \frac{\exp(i\vec{q}\vec{\rho})}{k_\parallel^2 - q^2}.$$

For the first integral, we return the switching of the variable,

$$q_\perp \to \tilde{q}_\perp = q_\perp \frac{k_\perp}{k_\parallel} \quad \text{and} \quad \rho_\perp \to \tilde{\rho}_\perp = \rho_\perp \frac{k_\perp}{k_\parallel},$$

to obtain

$$I_0(\vec{\tilde{\rho}}) = \frac{1}{8\pi^3 k_\perp^2}\int \frac{\exp(i\vec{\tilde{q}}\vec{\tilde{\rho}})}{\tilde{q}^2 - k_\perp^2} d^3\tilde{q} = \frac{1}{k_\perp^2} I_1(\vec{\rho}),$$

so

$$I_0(\vec{\tilde{\rho}}) = \frac{-1}{8\pi^3 k_\perp^2}\int_0^\infty \frac{1}{\tilde{q}^2 - k_\perp^2}\frac{\sin(\tilde{q}\tilde{\rho})}{\tilde{q}\tilde{\rho}} 4\pi q^2\, d\tilde{q} = \frac{-1}{2\pi^2 k_\perp^2 \tilde{\rho}}\int_0^\infty \frac{1}{\tilde{q}^2 - k_\perp^2}\sin(\tilde{q}\tilde{\rho})\tilde{q} d\tilde{q} d\tilde{q}$$
$$= \lim_{\varepsilon\to 0}\frac{i}{4\pi^2 k_\perp^2 \tilde{\rho}}\int_{-\infty}^\infty \frac{\exp(i\mu)}{\mu^2 - (k_\perp\tilde{\rho} + i\varepsilon)^2}\mu d\mu,$$

where $\mu = \tilde{q}\tilde{\rho}$ is taken based on the theorem of residue; it gives the following:

$$I_0(\tilde{\rho}) = \lim_{\varepsilon\to 0}\frac{i}{4\pi^2 k_\perp^2 \tilde{\rho}} 2i\pi \frac{k_\perp\tilde{\rho} + i\varepsilon}{2(k_\perp\tilde{\rho} + i\varepsilon)}\exp^{i(k_\perp\tilde{\rho} + i\varepsilon)} = \frac{-1}{4\pi k_\perp}\frac{\exp^{ik_\perp\tilde{\rho}}}{k_\perp\tilde{\rho}},$$

so

$$I_0(\tilde{\rho}) = \frac{-\exp\left(i\sqrt{k_\parallel^2\rho_\perp^2 + k_\perp^2\rho_z^2}\right)}{4\pi k_\perp\sqrt{k_\parallel^2\rho_\perp^2 + k_\perp^2\rho_z^2}} \quad \text{and} \quad I_1(\tilde{\rho}) = \frac{-1}{4\pi}\frac{\exp^{ik_\perp\tilde{\rho}}}{\tilde{\rho}}.$$

APPENDIX B: SIMPLIFICATIONS

We need to write $\frac{1}{\Delta}$, where $\Delta = (k_\perp^2 - q^2)(k_\parallel^2 k_\perp^2 - k_\parallel^2 q_z^2 - k_\perp^2 q_\perp^2)$.
We have two expressions:

$$\frac{1}{\Delta} = \frac{1}{(k_\perp^2 - q_z^2)(k_\parallel^2 - k_\perp^2)}\left[\frac{1}{k_\perp^2 - q^2} - \frac{k_\perp^2}{k_\perp^2 k_\parallel^2 - k_\parallel^2 q_z^2 - k_\perp^2 q_\perp^2}\right],$$

$$\frac{1}{\Delta} = \frac{1}{q_\perp^2(k_\parallel^2 - k_\perp^2)}\left[\frac{1}{k_\perp^2 - q^2} - \frac{k_\perp^2}{k_\perp^2 k_\parallel^2 - k_\parallel^2 q_z^2 - k_\perp^2 q_\perp^2}\right].$$

APPENDIX C: INTEGRAL FOR ϑ

$$I^1 = \int_0^{\frac{\pi}{2}} \cos\vartheta \sin\vartheta \sin(\tilde{n}\tilde{R}\cos\vartheta) d\vartheta,$$

$$I^2 = \int_0^{\frac{\pi}{2}} \sin\vartheta^3 \cos\vartheta \sin(\tilde{n}\tilde{R}\cos\vartheta) d\vartheta,$$

$$I^3 = \int_0^{\frac{\pi}{2}} \sin\vartheta \cos\vartheta^3 \sin(\tilde{n}\tilde{R}\cos\vartheta) d\vartheta.$$

Obviously we have

$$I^1 = I^2 + I^3,$$

or

$$I^1 = \frac{1}{\tilde{n}^2\tilde{R}^2}(\sin\tilde{n}\tilde{R} - \tilde{n}\tilde{R}\cos\tilde{n}\tilde{R}) = f^1(\tilde{n}\tilde{R}) = f^2(\tilde{n}\tilde{R}) + f^3(\tilde{n}\tilde{R}),$$

$$I^2 = \frac{2}{\tilde{n}^4\tilde{R}^4}(3\sin\tilde{n}\tilde{R} - 3\tilde{n}\tilde{R}\cos\tilde{n}\tilde{R} - \tilde{n}^2\tilde{R}^2) = f^2(\tilde{n}\tilde{R}),$$

$$I^3 = \frac{1}{\tilde{n}^4\tilde{R}^4}(-6\sin\tilde{n}\tilde{R} + 6\tilde{n}\tilde{R}\cos\tilde{n}\tilde{R} + 3\tilde{n}^2\tilde{R}^2\sin\tilde{n}\tilde{R} - \tilde{n}^2\tilde{R}^2\cos\tilde{n}\tilde{R}) = f^3(\tilde{n}\tilde{R}).$$

[1] J. Gal, Bull. Hist. Chem. **38**, No. 1 (2013).
[2] A. Eermin and A. Jakli, Soft Matter **9**, 615 (2013).
[3] G. Vertogen and W. H. de Jeu, *Thermotropic Liquid Crystals: Fundamentals* (Springer, Berlin, Heiderberg, 1988).
[4] S. Pieraccini, S. Masiero, A. Ferrarini, and G. Spada, Chem. Soc. Rev. **40**, 258 (2011).
[5] H. Coles and S. Morris, Nat. Photonics **4**, 676 (2010).
[6] S. Prosandeev, A. Malashevich, Z. Gui, L. Louis, R. Walter, I. Souza, and L. Bellaiche, Phys. Rev. B **87**, 195111 (2013).
[7] S. Zhong, Phys. Rev. Lett. **115**, 117403 (2015).
[8] V. P. Mineev and Yu. Yoshioka, Phys. Rev. B **81**, 094525 (2010).
[9] P. Hosur and X. L. Qi, Phys. Rev. B **91**, 081106(R) (2015).
[10] J. Orenstein and J. E. Moore, Phys. Rev. B **87**, 165110 (2013).
[11] N. Bitri, A. Gharbi, and J. P. Marcerou, Phys. B (Amsterdam, Neth.) **403**, 3921 (2008).
[12] Y. L. Geng and C. W. Qiu, IEEE Trans. Antennas Propag. **59**, 4364 (2011).
[13] H. de Vries, Acta Crystallogr. **4**, 219 (1951).
[14] D. W. Berreman, J. Opt. Soc. Am. **62**, 502 (1972).
[15] M. Zamani, H. N. Hajesmaeili, and M. H. Zandi, Opt. Mater. **58**, 38e45 (2016).
[16] L. Landau, L. Lifshitz, and L. P. Pitaevsky, *Electrodynamics of Continuous Media*, 2nd ed. (Pergamon Press, Oxford, 1984).
[17] For a review of the gyrotropic properties of helical conformations, see A. Lakhtakia, *Selected Papers on Natural Optical Activity* (SPIE Optical Engineering, Bellingham, WA, 1991).
[18] P. P. Crooker, *Chirality in Liquid Crystals*, edited by H. S. Kitzerow and C. Bahr (Springer, New York, 2001).
[19] P. Yeh, *Optical Waves in Layered Media* (Wiley, New York, 1988).
[20] P. G. de Gennes and J. Prost, *The Physics of Liquid Crystals*, 2nd ed. (Clarendon Press, Oxford, 1993).
[21] C. Oldano and M. Ratjeri, Phys. Rev. B **54**, 10273 (1996).
[22] P. Galatola, Phys. Rev. E **55**, 4338 (1997).
[23] J. Etxebarria, C. L. Folcia, and J. Ortega, Phys. Rev. E **64**, 011707 (2001).
[24] V. M. Agranovich and V. L. Ginzburg, *Spatial Dispersion in Crystal Optics and the Theory of Excitons*, 2nd ed. (Springer, Berlin, 1979).
[25] W. C. misner, S. K. Thorne, and J. A. Wheeler, *Gravitation* (W. H. Freeman, New York, 1970).
[26] F. Beaubois, J. P. Marcerou, H. T. Nguyen, and J. C. Rouillon, Eur. Phys. J. E **3**, 273 (2000).
[27] D. Bensimon, E. Domany, and S. Shtrikman, Phys. Rev. A **28**, 427 (1983).
[28] P. Allia, P. Galatola, C. Oldano, M. Rajteri, and L. Trossi, J. Phys. II France **4**, 333 (1994).
[29] R. Zgueb, H. Dhaouadi, and T. Othman, Liq. Cryst. **41**, 1394 (2014).